World Applied Sciences Journal 8 (8): 972-979, 2010
ISSN 1818-4952

Characterizations of Buried Silicon Nitride Layer Produced by Ion Implantation and Study its Electronic Properties.

[1]Majid Mojtahedzadeh Larijani and [2]Gholamhosain Haidari

[1]Agricultural medical and industrial research school, Karaj, Iran
[2]Department of Science, Malayer University, The fourth Km. of Malayer-Arak Road, Malayer, Iran, P.O.Box: 65719-95863

Abstract: Buried silicon nitride layers were produced by implanting ions with 90 Kev in <100> and <111> silicon at 500°C under high vacuum conditions. The stoichiometric Si/N ratio of 3/4 in the maximum of nitrogen depth distribution was adjusted by the fluence. The specimens were annealed at 950°C for three hours in order to investigate the influence of the annealing treatment on properties of the silicon nitride layers. Fourier transform infrared method (FT-IR) and X-ray diffraction (XRD) were used to analyze the silicon nitride layers. The electrical characteristics of the as-implanted and annealed SiN_x layers were analyzed with J-V measurements. It is found that this substrate temperature during ion implantation results in buried polycrystalline and dielectric silicon nitride layers. It was observed that the prevailing current conduction mechanism of as-implanted and annealed specimens is the Poole-Frenkel effect, as it is found also for silicon nitride prepared by other technologies. The results are compared with those obtained by ion implantation at room temperature to 400 °C and subsequence furnace annealing at higher temperature than 950 °C.

Key words: Ion implantation · Buried Silicon Nitride · Metal-Insulator-Semiconductor (MIS) · Furnace annealing

INTRODUCTION

Silicon nitride (SiN_x) layers are commonly used in micro electronics [1] where they may serve as dielectric insulators and diffusion barriers (e.g., against oxygen containing compounds and sodium), have masking properties and find a variety of applications as passive and active elements in electronic devices [2]. Their properties strongly depend on the preparation process [3, 4], deviation from stoichiometric N/Si ratio, present of impurities [5] and chemical bond state inside the layer [6-8]. The interest in thin silicon nitride layers produced by high dose nitrogen ions implantation into silicon (mainly single crystal silicon) has emerged due to their potential for application in silicon on insulator (SOI) technology [1,2]. These layers serve as protective oxidation and selective etching masks [1]. Silicon nitride layers produced by ion implantation are essentially impurity free (including hydrogen) and characterized by lower stress than those grown by several different chemical vapour deposition processes [9-12]. Formation of buried silicon nitride layers by ion implantation has been reported by several workers [13-16]. These workers have used ion implantation at room temperature to 400°C and subsequence conventional furnace annealing (FA). In general, a post-implantation thermal annealing at a temperature approximately 1200°C for duration of about 2 hours is necessary to synthesize crystalline buried silicon nitride layers. For ion implantation from room temperature to 400 °C, the as-implanted silicon nitride is amorphous and crystallization of silicon nitride starts only after annealing at 1200°C [14, 16]. In this paper, results on 90 Kev $^{14}N_2^+$ implantation at high fluence (10^{18} ions/cm^2) at substrate temperature of 500 °C followed by annealing (3h- 950°C) are reported and discussed. This means that, higher temperature during ion implantation and lower temperature during annealing than other ones, have chosen and the results are compared with each other [13-17]. Analyses have been made with FT-IR spectra and X-ray diffractograms. J-V measurements of as-implanted and annealed layers are discussed in order to investigate the dependence of the electronic characteristic of layers and the specimen treatment too.

Corresponding Author: Gholamhosain Haidari, Department of Science, Malayer University, The fourth Km. of Malayer-Arak Road, P.O.Box: 65719-95863 Malayer, Iran

Table 1: Specifications of different specimens.

No.	Silicon Substrate type	Fluence ...×10^{18} (ions/cm^2)	Annealing
A	(111)	0	---
B	(100)	0	---
1	(111)	0.76	---
2	(111)	1	---
3	(111)	1.18	---
4	(100)	1	---
5	(100)	0.76	v
6	(100)	1	v
7	(100)	1.18	v
8	(100)	1.5	v

Formation of Silicon Nitride Layers by Ion Implantation: By using calculations of the SRIM 2006 code, the mean projected range and standard deviation of 90 KeV Ni in Si are equal to 1176 A and 377 A, respectively. Therefore, doses about 10^{18} ions/cm^2 would be required to form a continuous Si_3N_4 layer. The HF etch cleaned single crystal Si wafers (<111> and <100>, R=1-30 Cm) were used as substrates. Silicon nitride layers were produced at 7° off the <100> and <111> directions by implanting $^{14}N_2^+$ ions with the energy of 90Kev and several fluences around 10^{18} ions/cm^2. During process of ion implantation, the substrate's temperature maintained at 500°C and the initial high vacuum conditions changed to the residual nitrogen gas pressure of 1.5×10^{-3} Pa. The MBM-100 system with ion beam current density of 45.3 μA /cm^2 was used.

Some implanted specimens were subsequently annealed in a conventional furnace at 950°C for three hours under nitrogen atmosphere of 10^{-2} mbar pressure.

Before metallization, the as-implanted and annealed specimens were chemically etched with HF/HNO_3 (1/5, room temperature for 20 S) in order to remove the Silicon-on-Insulator (SOI) layers.

Metal-Insulator-Semiconductor (MIS) capacitors were formed by physical vapour depositions method (DM-450A Coater PVD), as state bellow:

Pure aluminum was evaporated on the exposed buried silicon nitride layer and MIS capacitors were fabricated by defining square dots with the 5.7×10^{-3} cm^2 areas (thicknesses of 2000A) and using conventional photolithography technique. To ensure good Ohmic contact, Al metallization was also carried out on the backside of the specimens after removing the oxide.

Moreover, Al Ohmic contacts were formed by evaporating on the top and backside of the etched A and B specimens. Table 1 summarizes specifications of specimens.

RESULT AND DISCUSSION

Result and discussion of FT-IR and XRD analysis: The Tensor 27 (Bruker) spectrometer was used to record FT-IR spectra. Samples were also analyzed with an X-ray diffractometer (PW-1800(Philips)) using Cu and Co radiation (λ=1.54056 A and λ=1.78897 A).

FT-IR absorption spectra and X-ray diffraction for specimens 1, 2, 3 and 4 have been shown in Figure 1.a and Figure 1.b, respectively.

Si-N stretching bond in silicon nitride has wave number 800-900 cm^{-1} that depends on value of x/y in Si_xN_y [13-17]. A broad absorption band centered between 840 and 850 cm^{-1} in the Figure 1.a indicate x/y=3/4 [17]. There is another weak absorption peak centered at 875 cm^{-1} that indicate the crystallization of Si_3N_4 [14, 16]. In the Figure 1.b, there is a peak of silicon nitride (222) plane at 58.5° and was not observed peak for top damaged silicon. This is consistent with last result from the FT-IR study. This peak of silicon nitride doesn't appear for annealed specimens. It may be mentioned that Raurhan et al. [14] have observed the peak of top silicon (311) plane for the as-implanted samples but remained even after annealing up to 1250°C [16]. In our samples, this peak disappeared after the annealing process therefore this peak can not corresponding to (311) plane of top damaged silicon for as-implanted specimens.

There are a slight shift in the band position towards a higher wave number and additional peak as compared to 820 cm^{-1} for the sample implanted at a relatively low (250°C -340°C) substrate temperature [14]. This slight shift towards a higher wave number, additional peak and starts crystallization in our as-implanted samples, are attributed to the release of bound strains and disorder due to increased, evaluated substrate temperature (500°C) during ion implantation.

FT-IR absorption spectra for specimens 5, 6, 7 and 8 have been shown in Figure 2.a. Annealing leads to sharpening and a split of broad band into a complex spectrum consisting of three bands. The bands in the complex spectra are centered at 820 cm^{-1}, 880 cm^{-1} and 915 cm^{-1}. The center-band positions at 845 cm^{-1}, 890 cm^{-1} and 945 cm^{-1} for furnace annealing at 1200°C - 3h are reported by Ruthann et al [14]. Here also the shift towards higher wave number is attributed to a further release of bond strains and disorder (introduced by implantation) due to annealing. The complex spectrum is related to the crystalline nature of the buried silicon nitride [16]. X-ray diffractograms for specimens 5, 6, 7 and 8 are shown in Figure 2.b. The peak corresponding to (222) plane

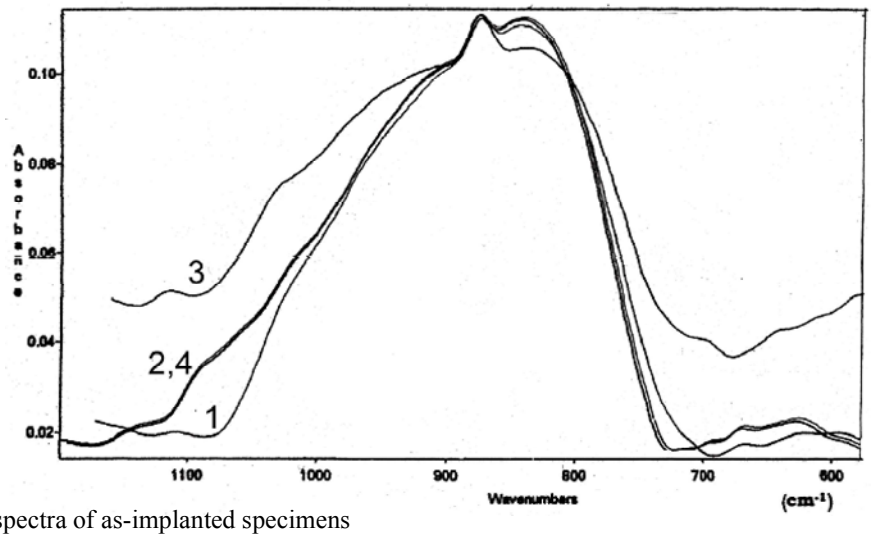

Fig. 1.a: FT-IR spectra of as-implanted specimens

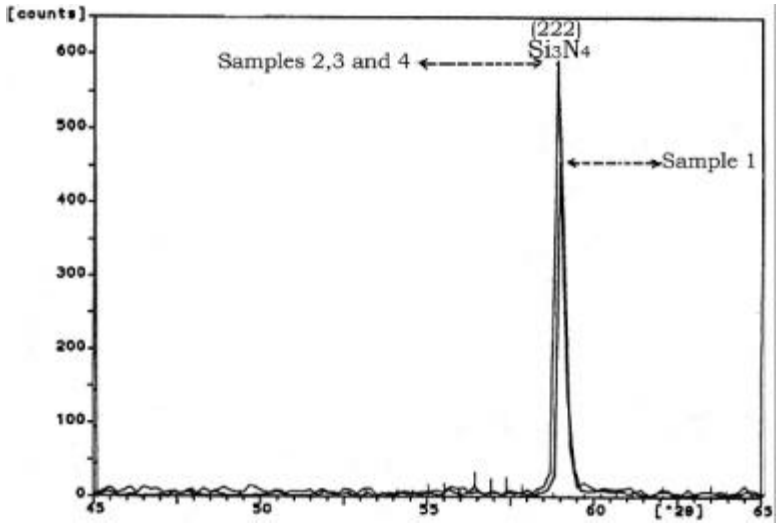

Fig. 1.b: XRD spectra of as-implanted specimens

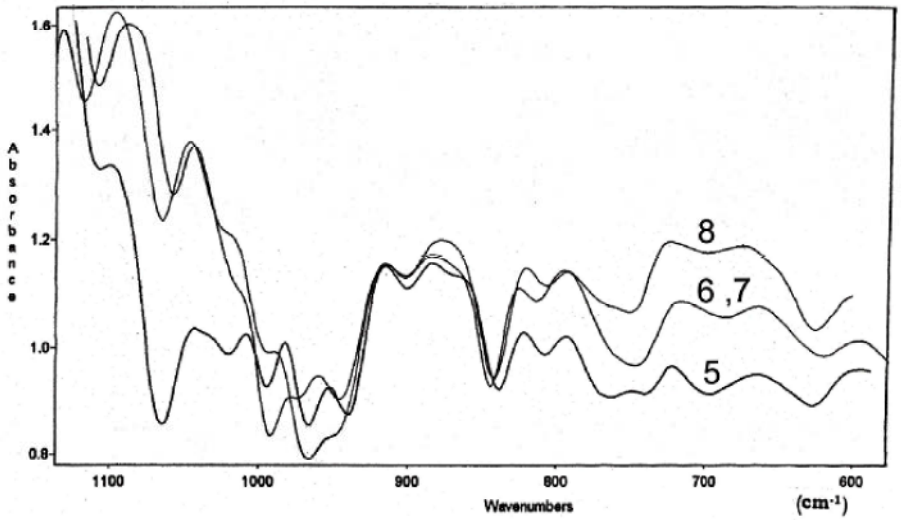

Fig. 2.a: FT-IR spectra of annealed specimens.

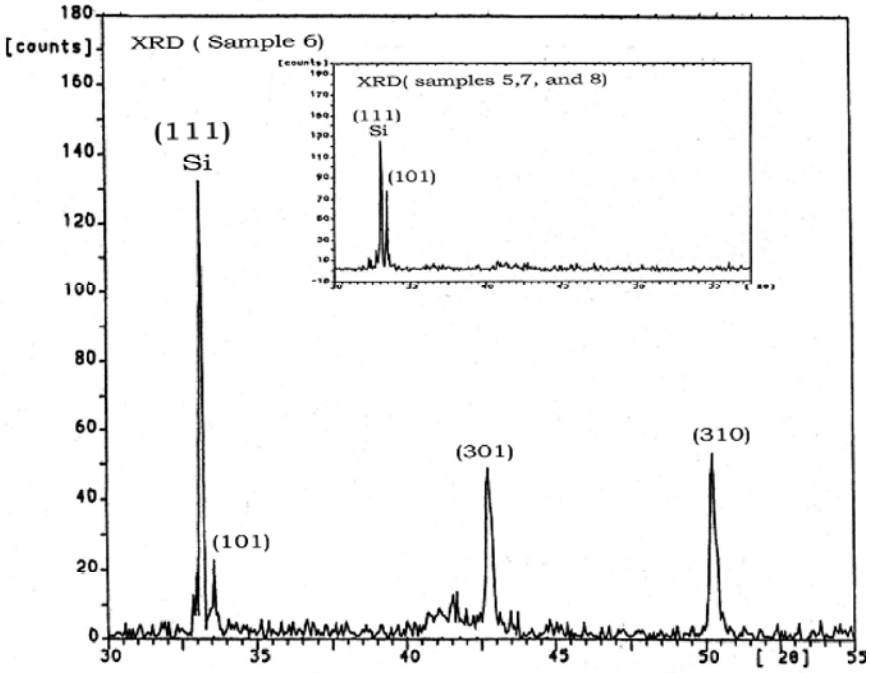

Fig. 2.b: XRD spectra of annealed specimens

Table 2: Experimental results of XRD

No.	*Diameter (Angstrom) ˜d(A)*						
A	3.13	1.04	----	----	----	----	----
B	----	----	1.35	----	----	----	----
1,2,3 and 4	----	----	----	1.58	----	----	----
5	----	----	----	----	2.67	----	----
6	----	----	----	----	2.67	2.10	1.82*
7	----	----	----	----	2.67	2.10*	1.82
8	----	----	----	----	2.67	2.10*	1.82

* The intensity of this peak is weak.

Table 3: Reference values for silicon and silicon nitride (ASTM Standard*)

d(A)	*(hkl)*	*Type*
3.138	(111)	Silicon
1.045	(511)	Silicon
1.357	(400)	Silicon
1.638	(311)	Silicon
1.596	(222)	Silicon Nitride
2.669	(101)	Silicon Nitride
2.083	(301)	Silicon Nitride
1.827	(310)	Silicon Nitride

* American Society for Testing and Materials

disappears while a few other emerge. For specimen "six" (101), (301) and (310) planes corresponding to α-Si_3N_4 emerge. Appearance of (111) peak linked to top silicon after annealing is attributed to the recrystalliszation of top damaged silicon into polysilicon. The other workers with different conditions of ion implantation and annealing methods have also observed almost same planes of α-Si_3N_4 and top silicon with difference in intensity of peaks [14-16]. These XRD results and ASTM standard data are shown in Table 2 and 3.

J-V measurements: The J-V characteristics of the SiN_x layers were measured with an accurate voltage and ampere meter.

Silicon nitride prepared by different technologies like Chemical Vapour Deposition (CVD) [18], Low pressure CVD (LPCVD) [19], Plasma Enhanced CVD (PECVD) [19-21] or nitrogen glow discharge [22] all exhibit a typical J-V characteristic with an Ohmic behavior for low electric field strength and current conduction Poole–Frenkel effect for high fields and seems to be a universal property of this material [23]. The Ohmic branch is usually ascribed to the hopping of thermally excited electrons from one trap state to another.

The Poole–Frenkel effect is explained as subsequence trapping of electrons and field-enhanced thermal re-emission into the conduction band [18]. In this work, the measured J-V characteristics were fitted using the relation

$$J_{ohmic}=E/\rho \quad (1)$$

for the Ohmic branch with resistivity ρ and

$$\frac{J_{P-F}}{E}=Cons.\times\exp\left\{\frac{q}{KT}\sqrt{\frac{q}{\Pi\varepsilon_s\varepsilon_d}}\sqrt{E}\right\} \quad (2)$$

for the Poole-Frenkel branch with dynamic dielectric constant ϵ_d in order to find out if the sum of both contributions:

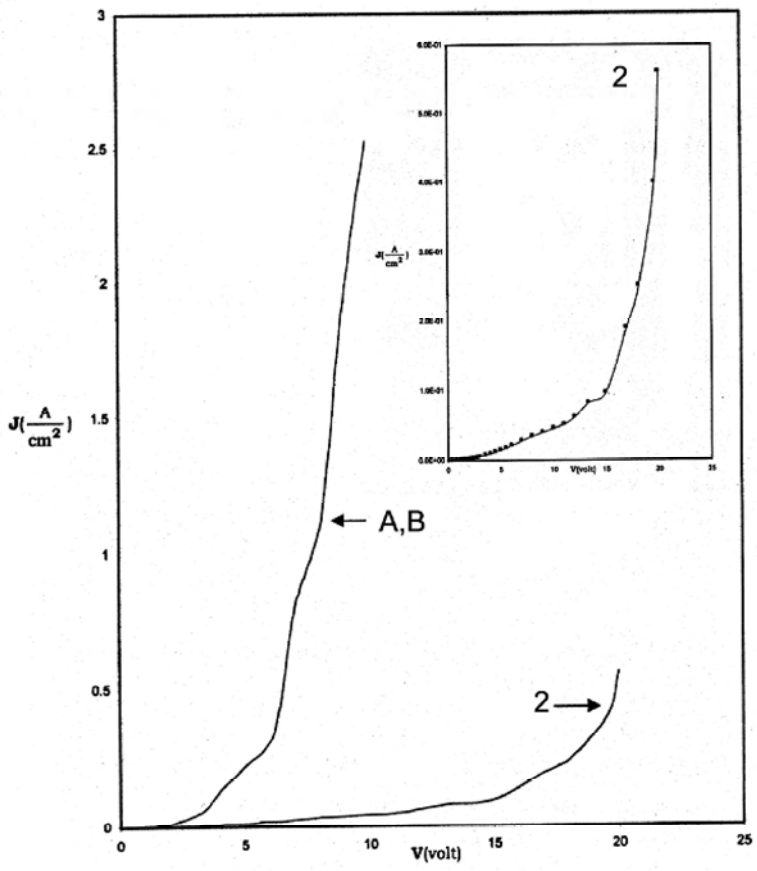

Fig. 3: J-V characteristics of MIS capacitors of specimen A, B and 2

$$J_{total}=J_{ohmic}+J_{p-f} \quad (3)$$

also describe the current conduction behavior of the implanted SiN_x layers in a satisfactory manner.

The J-V characteristics were plotted in a Poole-Frenkel diagram (logarithm of conductivity J/E versus $\sqrt{E}$), where the Ohmic branch appears horizontal and the Poole-Frenkel branch as an ascending line. From the slope of the latter the dynamic dielectric constant ϵ_d of the SiN_x can be derived from equation (2). According to the relation

$$\epsilon_d=n^2 \quad (4)$$

the refractive index can be estimated. A proper value of "n" confirms self-consistently the occurrence of the Poole–Frenkel effect.

Results and Discussion of J-v Measurement: Figure 3 shows the J-V characteristics of specimen A, B and 2. This figure reflects that a reasonable dielectric of the buried silicon nitride layer exists across specimen 2. The J-V characteristics in Poole-Frenkel diagram of specimen 2 and 6 are shown in Figure 4 and Figure 5. According to figure 4 and figure 5, the break down voltage of specimen 2 is 20v (breakdown field strength is2.35×10^6 v/cm) and increase to 55v (breakdown field strength is 5.8×10^6 v/cm) for the specimen 6. Comparably low dielectric strength of the implanted SiN_x can be partly explained with the non-abrupt nitrogen distribution over the implantation depth [23-25]. Another result of the annealing treatment is the shift of the onset of the Poole-Frenkel effect towards higher electrical field strengths.

Both as-implanted and annealed samples show the typical Si_3N_4 J-V characteristics with Ohmic behavior for low electric fields and Poole-Frenkel effect for high fields. It is very difficult to interpret these J-V curves at very low electric fields (e.g. up to 0.25 Mv/cm for annealed sample) as they are very complicated due to low current values and long transients [25]. The two classes of J-V characteristics measured for the as-implanted and annealed samples can be explained by a partial appearance of small structure on the specimens surface [23,24]. The sums of the two contributions (Solid curves

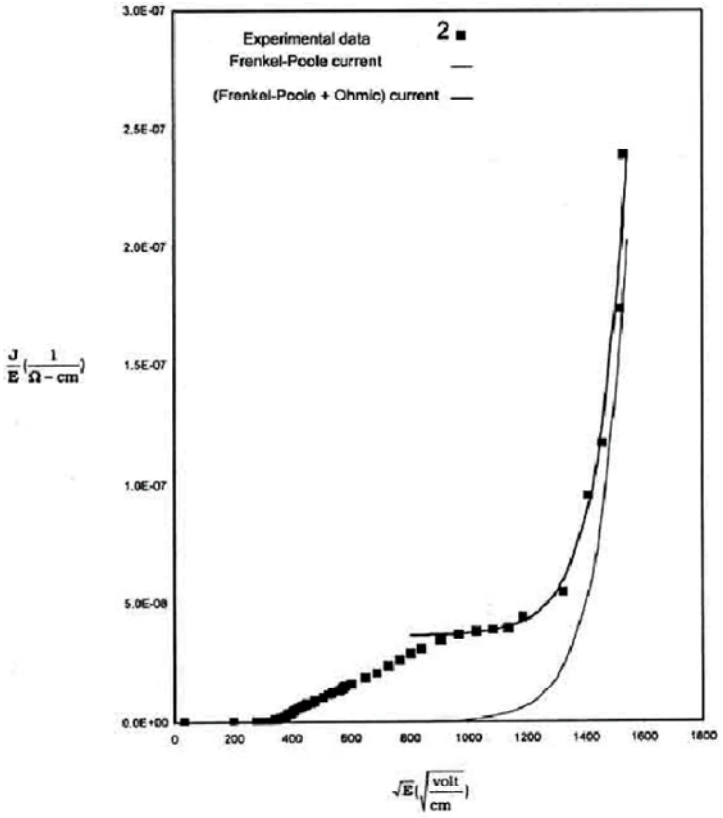

Fig. 4: J-V characteristics of MIS capacitor of specimen 2 in Poole-Frenkel diagram

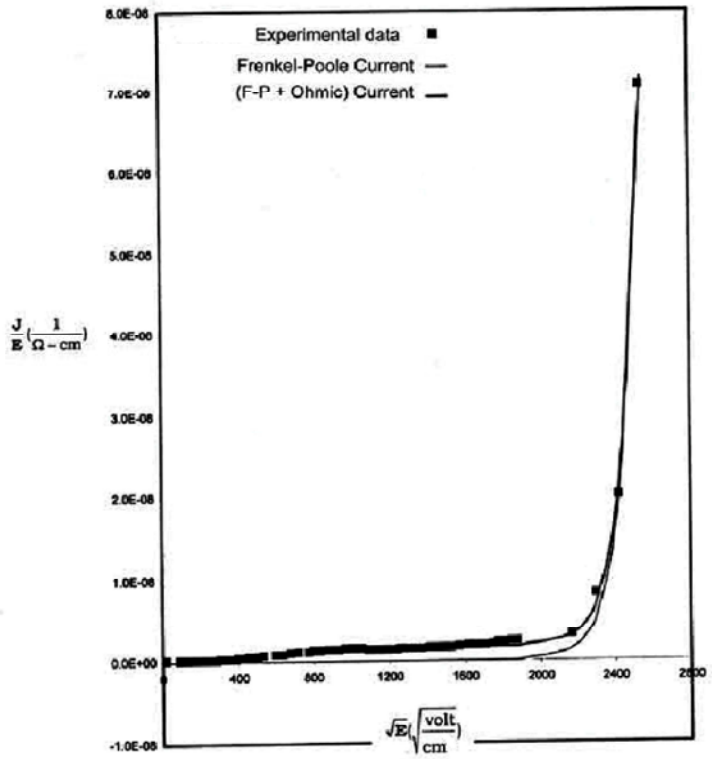

Fig. 5: J-V characteristics of MIS capacitor of specimen 6 in Poole-Frenkel diagram

in Figure 4 and Figure 5) fit the measured characteristics well. By Figure 4 and Figure 5, the specific resistance of the as-implanted specimen is $\rho = 2.5\times10^{8}\Omega$ - cm and increased to $\rho = 1\times10^{9}\ \Omega$ - cm for the annealed specimen, respectively. Some workers have reported that the as-implanted layer does not show a distinct electrical breakdown due to its low resistance [23]. This J-V characteristic for as-implanted specimen is due to increased substrate temperature (500°C) during ion implantation. The specific resistances for annealed specimens are found lower than the values reported by other workers [23,24]. This is due to annealing at 950°C-3h. It was shown by Markwitz et al [24] that an annealing treatment (1200°C) in a conventional furnace for one hour led to a decrease of the current flow through the SiN_x layers but when the annealing time exceeded two hours, the electrical properties deteriorated.

From the Poole-Frenkel branch fit the dynamic relative dielectric constant of the annealed specimen (figure 5) can be derived to be about $\varepsilon_d = 7.2$. This yields a refractive index of n=2.7, which is somewhat higher than the expected value of 2.05 for Si_3N_4.

Moreover, the high frequency C-V characteristics of the MNS capacitor were measured at 1 MHz to characterize the buried Si3N4-Si substrate interface. This does not show any modulation in the capacitance value for an applied voltage in the range from -60V to +60V. A similar behavior was also reported for the MNS capacitance fabricated on the SOI substrate, synthesized under almost similar conditions [25,26]. One of the most likely reasons for such a C-V behavior seems to be the presence of very high charge density at the lower Si_3N_4-Si interface due to which bulk electrode behaves like a metallic contact.

CONCLUSION

FT-IR spectra demonstrated that polycrystalline Si_3N_4 could be synthesized by nitrogen ion implantation at substrate temperature of 500°C. XRD analysis also showed the crystalline structure of as-implanted and annealed specimens. It was observed that the prevailing current conduction mechanism of as-implanted and annealed specimens is the Poole-Frenkel effect, as it is found also for silicon nitride prepared by other technologies. In contrast with ion implantation at room temperature to 400°C and then annealing higher temperature than 950°C, substrate temperature of 500°C can be helpful to achieve crystalline and dielectric buried silicon nitride, but lower annealing temperature (3h-950°C), does not lead to proper specifications.

ACKNOWLEDGEMENTS

The authors wish to express their thanks to all staff of Ionic beams Center and Malayer University for making these works possible.

REFERENCES

1. Krimmelk, E.F., 1991. Co-operation in: Gmelin Handbook of Inorganic and Organometallic Chemistry Si; Supplement B 5C Silicon Nitride in Microelectronics, Springer, Heidelberg.
2. Ito, I., I. Kato, T. Nakamura and H. Ishikawa, 1983. Proceedings of the Symposium on Si_3N_4 thin films, 83(3): 295.
3. Mort, J. and E. Jansen, 1986. Plasma Deposited Thin Films, Boca Raton: CRC Press.
4. Markwitz, A., H. Baumann, W. Grill, E.F. Krimmel and K. Bethge,1994. Appl. Phys. Lett., 64: 2652.
5. Markwitz, A., H. Baumann, P. Misaelides, E.F. Krimmel and K. Bethge Fresenius,1993. J. Anal. Chem., 346: 177.
6. Markwitz, A., H. Baumann, E.F. Krimmel, R.W. Michelmann, C. Maurer, E.C. Paloura, A. Knop and K. Bethge, 1994. Appl. Phys. A., 59: 435.
7. Markwitz, A., H. Baumann, W. Grill, B. Heinz, A. Roseler, E.F. Krimmel and K. Bethge, Fresenius, 1995. J. Anal. Chem., 353: 734.
8. Michelmann, R.W., H. Baumann, A. Markwitz, J.D. Meyer, A. Roseler, E.F. Krimmel and K. Bethge, Fresenius,1995. J. Anal. Chem., 353: 403.
9. Hemment, P.L.F., R.F. Peart, M.F. Yao, K.G. Stephens, R.J. Chater, J.A. Kilner, D. Meekison, G.R. Booker and R.P. Arrowsmith, 1985. Phys. Rev. Lett., 46: 952.
10. Reeson, K.J., P.L.F. Hemment, C.D. Meekison, G.R. Booker, J.A. Kilner, R.J. Chater, J.R. Davis and G.K. Celler, 1987. Appl. Phys. Lett., 50: 1882.
11. Reeson, K.J., 1987. Nucl. nstr. And Meth. B 19/20: 269.
12. Skorupa, W., K. Wollschlager, U. Kreissig, R. Gotzschel and H. Bartsch, 1987. Nucl. Instr. And Meth. B 19/20: 285.
13. Tsujide, T., M. Nojiri and H. Kitagawa, 1980. J. Appl. Phys., 51(3): 1605.
14. Rauthan, C.M.S., A. Chand, S. Chandra and G. Bose, 1987. Thin Solid Film, 165: 429.
15. Bourguet, P., J.M. Dupart, E. Le. Tiran, P. Auvray, A. Guivarch, M. Salvi, G. Pelous and P. Henoc, 1980. J. Appl. Phys., 51(12): 6169.
16. Vird, G.S., C.M. Rautahn, B.C. Pathak and W.S. Khokle, 1992. Appl. Phys. Lett., 60(4)27: 492.

17. Speakman, S.P., P.M. Read and A. Kiermasz, 1988. Vacuum, 38: :3183.
18. Sze, S.M., 1976. J. Appl. Phys., 38: 2951.
19. Parsons, G.N., J.H. Souk and J. Batey, 1991. J. Appl. Phys., 76: 1553.
20. Hsieh, S.W., C.Y. Chang, Y.S. Lee, C.W. Lin and S.C. Hsu, 1994. J. Appl. Phys., 76: 3645.
21. Paloura, E.C., J. Lagowski and H.C. Gatos, 1991. J. Appl. Phys., 69(7): 3995.
22. Markwitz, A., M. Arps, H. Baumann, E.F. Krimmel and K. Bethge, 1996. Nucl. Instr. And meth. In phys. Res., B 113: 223.
23. Markwitz, A., M. Arps, H. Baumann, G. Demortier, E. F. Krimmel and K. Bethge, 1997. Nucl. Instr. And meth. In phys. Res., B 124: 506.
24. Rauthan, C.M.S., G.S. Viridi, B.C. Pathak and A. Karthigeyan, 1998. J. Appl. Phys., 83-7: 3668.
25. Zimmer, G., W. Zetzmann, Z.L. Liu and E. Neubert, 1983. Ion Implantation Techniques, Berlin: Springer, pp: 426.